LETTER

Synaptotagmin 7 confers frequency invariance onto specialized depressing synapses

Josef Turecek[1]*, Skyler L. Jackman[1]* & Wade G. Regehr[1]

At most synapses in the brain, short-term plasticity dynamically modulates synaptic strength. Rapid frequency-dependent changes in synaptic strength have key roles in sensory adaptation, gain control and many other neural computations[1,2]. However, some auditory, vestibular and cerebellar synapses maintain constant strength over a wide range of firing frequencies[3–5], and as a result efficiently encode firing rates. Despite its apparent simplicity, frequency-invariant transmission is difficult to achieve because of inherent synaptic nonlinearities[6]. Here we study frequency-invariant transmission at synapses from Purkinje cells to deep cerebellar nuclei and at vestibular synapses in mice. Prolonged activation of these synapses leads to initial depression, which is followed by steady-state responses that are frequency invariant for their physiological activity range. We find that synaptotagmin 7 (Syt7), a calcium sensor for short-term facilitation[7], is present at both synapses. It was unclear why a sensor for facilitation would be present at these and other depressing synapses. We find that at Purkinje cell and vestibular synapses, Syt7 supports facilitation that is normally masked by depression, which can be revealed in wild-type mice but is absent in Syt7 knockout mice. In wild-type mice, facilitation increases with firing frequency and counteracts depression to produce frequency-invariant transmission. In Syt7-knockout mice, Purkinje cell and vestibular synapses exhibit conventional use-dependent depression, weakening to a greater extent as the firing frequency is increased. Presynaptic rescue of Syt7 expression restores both facilitation and frequency-invariant transmission. Our results identify a function for Syt7 at synapses that exhibit overall depression, and demonstrate that facilitation has an unexpected and important function in producing frequency-invariant transmission.

One reason why it is difficult to maintain constant synaptic strength is that during high-frequency presynaptic activation there is little time to replenish vesicles, and synaptic strength decreases as vesicle depletion becomes more severe (Extended Data Fig. 1a, c). Consequently, many synapses depress to a greater extent as activation frequency increases[8–10]. This property can be used computationally as a dynamic gain control mechanism[1]. Despite the challenges posed by vesicle depletion, some synapses transmit faithfully across a wide range of activation frequencies[3–5] (Extended Data Fig. 1b, d–f). In the vestibular system, such frequency-invariant transmission effectively conveys the absolute firing rate of vestibular afferents, and contributes to the linearity of occulomotor reflexes[4]. Several mechanisms have been proposed to explain how synapses could maintain frequency-invariant transmission[3,5,11], but the molecular tools to address these models directly have been lacking. Here we test the hypothesis that facilitation, a short-lived increase in the probability of release (P_R), counteracts vesicle depletion to produce frequency-invariant transmission (Extended Data Fig. 1d). We take advantage of the recent finding that genetic knockout of the slow synaptotagmin isoform Syt7 selectively eliminates facilitation at some synapses[7].

We began by studying synapses made by Purkinje cells (PCs), the sole output neurons of the cerebellar cortex, which fire spontaneously at 10–120 Hz in vivo[12]. Purkinje cells form GABA (γ-aminobutyric acid)-releasing synapses in the deep cerebellar nuclei (DCN, Fig. 1a), and express Syt7 (Fig. 1b). The presence of Syt7 was intriguing because, unlike many synapses with prominent Syt7 expression, PC–DCN synapses depress. We found that Syt7 expression at PC–DCN synapses is age-dependent, unlike expression of the PC marker calbindin and Syt2 (Extended Data Fig. 2). The onset of Syt7 expression is correlated with the development of frequency-invariant transmission at PC–DCN synapses (Fig. 1c–f and Extended Data Figs 3, 4). In young animals (postnatal day (P)13–15), Syt7 expression is low, and steady-state transmission is frequency-dependent in both wild-type and Syt7 knockout mice (Fig. 1c–e, left). Syt7 expression increases in juvenile wild-type mice (P21–32), and transmission becomes more frequency-invariant with age. However, in juvenile Syt7 knockout mice, frequency-invariant transmission does not develop (Fig. 1c–e, middle). The differences between wild-type and knockout mice become more pronounced in adulthood (Fig. 1c–e, right). As a consequence, synaptic charge transfer (the product of inhibitory postsynaptic current (IPSC) amplitude and activation frequency) becomes more linear during development in wild-type mice, but remains sublinear in Syt7 knockout mice (Fig. 1f). These findings indicate that Syt7 is required for frequency-invariant transmission at PC–DCN synapses.

To determine what caused the loss of frequency-invariant transmission in Syt7 knockout mice, we examined recovery from depression, the initial P_R, and facilitation. Syt7 mediates rapid calcium-dependent recovery from depression in cultured hippocampal synapses[13]. One possibility is that Syt7 contributes to frequency-independent transmission by accelerating recovery from depression during high-frequency activity (Extended Data Fig. 1e). Recovery from depression would then be faster in wild-type mice than in Syt7 knockout mice; however, this was not the case (Extended Data Fig. 5). Syt7 also mediates asynchronous release during high-frequency stimulation at some synapses[14,15], but asynchronous release is not prominent at PC–DCN synapses (Extended Data Fig. 6).

We also tested the hypothesis that P_R is elevated in Syt7 knockout mice. If P_R were increased, stronger depletion could more effectively mask facilitation and lead to a loss of frequency-invariant transmission[6]. An increase in P_R would be expected to increase the size of PC inputs, but we found no significant difference in single fibre size between wild-type and Syt7 knockout mice (Extended Data Fig. 7). We lowered external calcium (Ca_e) to decrease P_R and reduce the masking effects of vesicle depletion, and found that at PC–DCN synapses facilitation was prominent in wild-type mice, but weak or absent in Syt7 knockout mice (Fig. 2a). If the loss of frequency-independent transmission is a consequence of an increase in P_R, then reducing P_R by lowering Ca_e should lead to frequency-invariant transmission in Syt7 knockout mice. However, when Ca_e was lowered from 1.5 mM (control) to 1 or 0.5 mM

[1]Department of Neurobiology, Harvard Medical School, 220 Longwood Avenue, Boston, Massachusetts 02115, USA.
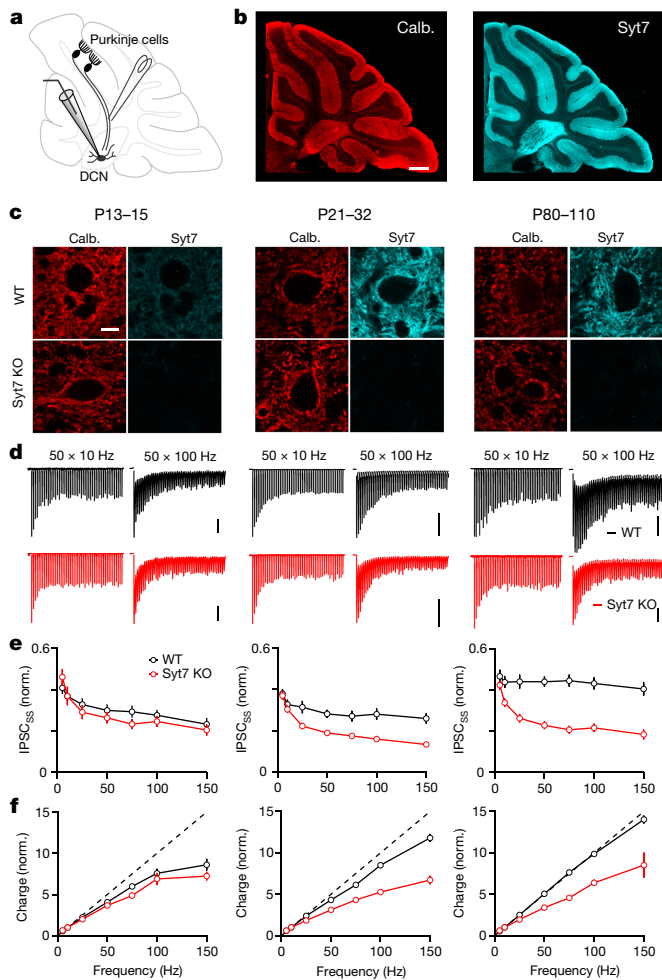*These authors contributed equally to this work.

Figure 1 | Syt7 is required for frequency-invariant transmission at PC–DCN synapses. a, PC axons were stimulated and responses were recorded from DCN projection neurons. **b**, Sagittal cerebellum from a wild-type mouse at postnatal day 25 (P25) immunolabelled for calbindin (left) and Syt7 (right). Scale bar, 0.5 mm. **c**, High-power images of the DCN immunolabelled for calbindin and Syt7 from young (left, P13–15), juvenile (middle, P21–32), and adult (right, P80–110) wild-type (WT) and Syt7 knockout (KO) mice. Scale bar, 10 μm. **d**, Representative IPSCs for wild-type (black) and Syt7 knockout mice (red) for young (left), juvenile (middle) and adult (right) mice. Stimulus artefacts have been blanked for clarity. Vertical scale bars, 1 nA. **e**, Normalized steady-state amplitudes (IPSC$_{SS}$) as a function of stimulation frequency for young (left), juvenile (middle) and adult (right) mice. **f**, Charge transfer calculated as the product of IPSC$_{SS}$ amplitude and stimulation frequency for young (left), juvenile (middle) and adult (right) mice. Data are mean ± s.e.m. Number of experiments shown in Extended Data Table 1.

to reduce IPSC amplitudes to 42% and 12% of control, respectively[5], transmission in Syt7 knockout mice remained frequency-dependent (Fig. 2b, c). These results indicate that the loss of frequency invariance in Syt7 knockout mice does not result from an increase in initial P_R.

We next looked for evidence of facilitation at physiological levels of Ca$_e$ (1.5 mM). Facilitation was measured by first using stimulation at 10 Hz to induce baseline depletion, and then increasing the frequency to 100 Hz[5,16]. In wild-type mice, frequency steps revealed a transient enhancement with a magnitude that was correlated with the development of frequency-invariant transmission (Fig. 2d). These results are consistent with facilitation leading to sustained increases in P_R that are transiently revealed until they are masked by vesicle depletion. In Syt7 knockout mice, facilitation was not observed at any age, and increases in stimulus frequency depressed IPSCs. Thus, Syt7-dependent facilitation is prominent when transmission is frequency independent
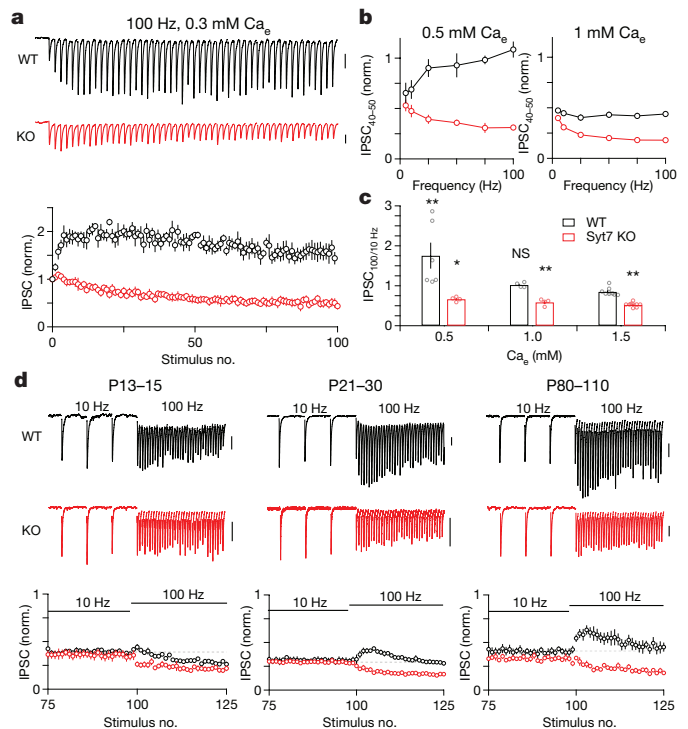

Figure 2 | Syt7 is required for a hidden form of facilitation at PC–DCN synapses. a, Experiments were conducted in P21–32 mice in low Ca$_e$ (0.3 mM) to reduce the initial probability of release. Responses are shown for representative experiments (top) and summarized across experiments (bottom). **b**, Average of 40th–50th IPSCs as a function of stimulation frequency. **c**, Ratio of IPSC$_{SS}$ induced by 100-Hz and 10-Hz (IPSC$_{100/10 \text{ Hz}}$) stimulation in different Ca$_e$. **d**, PC synapses were stimulated in 1.5 mM Ca$_e$ at 10 Hz to reach steady-state, followed by 100 Hz stimulation in young (left), juvenile (middle) and adult (right) mice. Example responses (top) and summaries (bottom) are shown. Stimulus artefacts have been blanked for clarity. Vertical scale bars, 0.25 nA. *$P < 0.05$, **$P < 0.01$, one-way ANOVA with Tukey's post-hoc test. Data are mean ± s.e.m. Number of experiments shown in Extended Data Table 1.

(juvenile and adult wild-type mice), and is weak when transmission is frequency dependent (young wild-type mice and Syt7 knockout mice of all ages).

To determine whether impaired frequency-invariant transmission was due specifically to presynaptic loss of Syt7[17], we performed rescue experiments in global Syt7 knockout mice. We used adeno-associated viruses (AAVs) to express yellow-fluorescent protein-tagged channel-rhodopsin 2 (ChR2–YFP) alone, or to bicistronically express both Syt7 and ChR2–YFP presynaptically[7] (Fig. 3a). However, it is not possible to obtain expression in all PCs, and it is impractical to optically stimulate axons at high frequencies for prolonged trains[18]. We therefore used optical stimulation to identify ChR2-expressing fibres that could be isolated electrically (Fig. 3b, c). These axons were then electrically stimulated at a high frequency. In Syt7 knockout mice, facilitation was absent in axons expressing ChR2–YFP alone, but was prominent in fibres expressing both ChR2–YFP and Syt7 (Fig. 3d). Steady-state transmission was nearly constant when Syt7 was expressed, but remained frequency-dependent when only ChR2–YFP was present (Fig. 3e, f). Consequently, charge transfer in Syt7-expressing PC axons was linear, but remained sub-linear when only ChR2–YFP was expressed (Fig. 3g-h). Viral expression of Syt7 allowed PCs in Syt7 knockout mice to become as frequency invariant as in wild-type mice (Fig. 3h), indicating that presynaptic Syt7 mediates frequency-invariant transmission.

Having established that Syt7 is required for frequency invariance in PC synapses, we investigated whether Syt7 plays a similar role at vestibular synapses. Afferents from the vestibular ganglion project
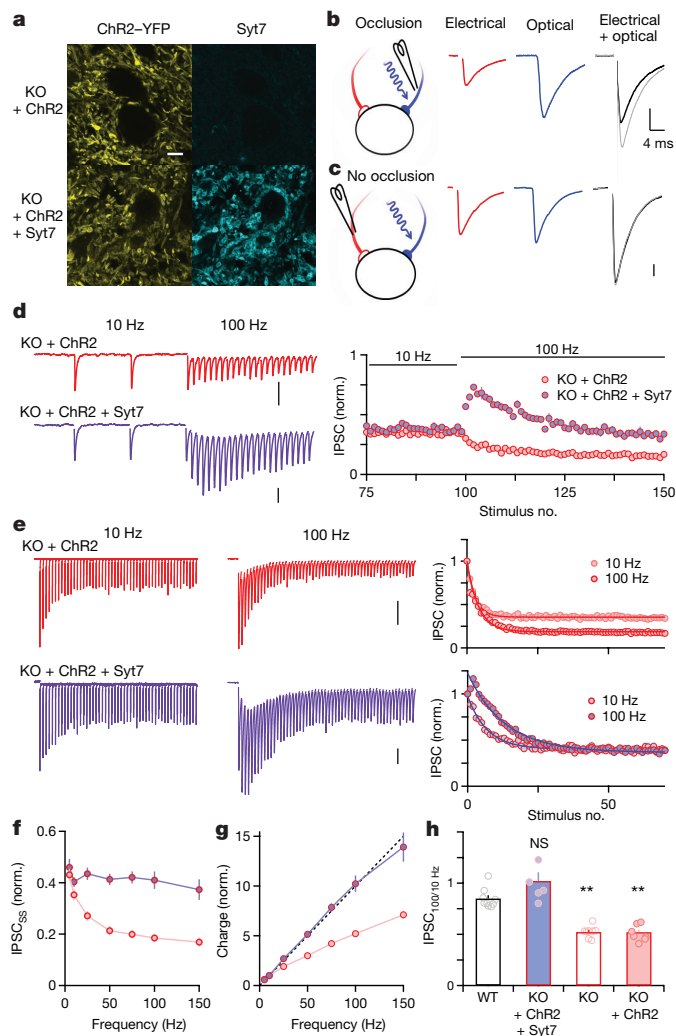
Figure 3 | Presynaptic expression of Syt7 restores facilitation and frequency-invariant transmission at PC–DCN synapses in Syt7 knockouts. a, ChR2–YFP fluorescence and Syt7 immunolabelling in the DCN of Syt7 knockout mice following AAV-driven expression of either ChR2–YFP alone (top) or ChR2–YFP and Syt7 (bottom) in PCs. Scale bar, 10 μm. **b**, **c**, The ability of IPSCs evoked electrically and optically to occlude each other was used to identify labelled fibres. **b**, If PC fibres express ChR2, the algebraic sum of electrical (red) and optical (blue) stimulation (grey) exceeds responses evoked by simultaneous optical and electrical stimulation (black). **c**, If electrically stimulated axons do not express ChR2, the sum of optical and electrical responses (grey) matches responses evoked by simultaneous optical and electrical stimulation (black). Vertical scale bars, 0.5 nA (**b**, **c**). **d**, PC axons expressing ChR2–YFP alone (red) or ChR2–YFP and Syt7 (purple) were electrically stimulated at 10 Hz and then 100 Hz. **e**–**g**, PC inputs were stimulated at 5–150 Hz for ChR2–YFP alone (red) or ChR2–YFP and Syt7 (purple). **e**, Responses evoked by trains. Stimulus artefacts have been blanked for clarity. Vertical scale bars, 1 nA (**d**, **e**). **f**, Average steady-state responses versus stimulation frequency. **g**, Charge transfer as a function of stimulation frequency. **h**, Summary of ratios of IPSC$_{SS}$ amplitudes at 100 Hz and 10 Hz. **$P < 0.01$, one-way ANOVA with Tukey's post-hoc test. Data are mean ± s.e.m. Number of experiments shown in Extended Data Table 1.

to the magnocellular medial vestibular nucleus (MVNm, Fig. 4a). Syt7 is expressed in the neuropil of the MVNm, where vestibular afferents form glutamatergic synapses (Fig. 4b). Although previous studies did not report facilitation at this synapse[11], we found that vestibular synapses show facilitation at low levels of Ca$_e$ in wild-type but not Syt7 knockout mice (Fig. 4c). At physiological levels of Ca$_e$, step changes in stimulation frequency produced transient enhancement in wild-type but not Syt7 knockout mice (Fig. 4d). These responses suggest that
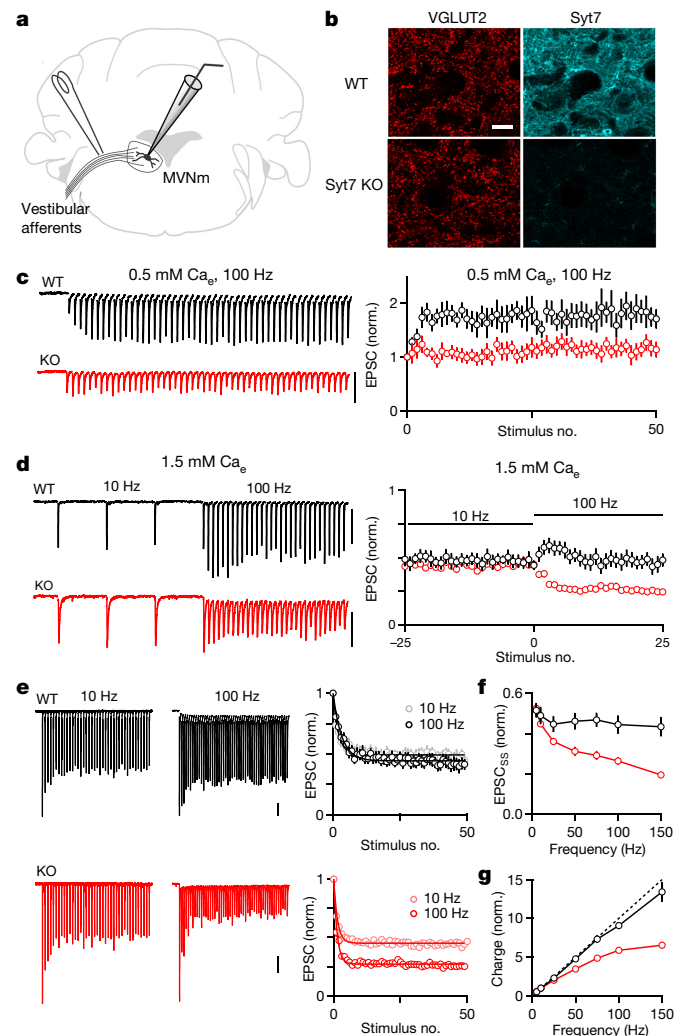

Figure 4 | Syt7 is also required for frequency-invariant transmission at vestibular synapses. a, Schematic showing stimulus electrode placement to activate vestibular afferents while recording from MVNm neurons. **b**, Immunofluorescence for VGLUT2 (left) and Syt7 (right) surrounding MVNm cells in P25 mice. Scale bar, 20 μm. **c**, Responses evoked by stimulating vestibular afferents in 0.5 mM Ca$_e$. **d**, Vestibular inputs were stimulated at 10 Hz, followed by 100 Hz in 1.5 mM Ca$_e$. **e**–**g**, Vestibular inputs were stimulated with 5–150-Hz trains in 1.5 mM Ca$_e$ in wild-type and Syt7 knockout mice. **e**, Representative (left) and average (right) EPSCs evoked by trains. **f**, Average steady-state responses against stimulation frequency. **g**, Charge transfer as a function of stimulation frequency. Stimulus artefacts have been blanked for clarity. Vertical scale bars, 0.1 nA. Data are mean ± s.e.m. Number of experiments shown in Extended Data Table 1.

Syt7-mediated facilitation is also present at vestibular synapses, but is masked by depletion. We also found that steady-state transmission was frequency-invariant and charge transfer was linear in wild-type but not Syt7 knockout mice (Fig. 4e–g, Extended Data Fig. 8).

We have shown that Syt7 mediates a hidden component of facilitation that counteracts partial vesicle depletion to produce linear charge transfer. Synaptic properties in wild-type and Syt7 knockout mice conform to a model in which the loss of frequency-invariance in Syt7 knockout mice is accounted for by the absence of facilitation[5] (Extended Data Fig. 9). Linear charge transfer and Syt7 expression at PC synapses emerge during development, but for technical reasons most synapses have been studied only in young animals[19]. The prevalence of frequency-invariant transmission in adults is unknown, but indirect measurements *in vivo* suggest that it may be widespread[20,21]. Moreover, Syt7 is developmentally regulated[22,23] and widely expressed in the adult brain, often in cells that make depressing synapses[22,24]. The kinetics

of Syt7 make it well suited to operate within the physiological firing range of PCs and vestibular afferents[4,12,25,26]. While our results show that linear charge transfer is mediated by Syt7 at PC and vestibular synapses, other synapses may use different mechanisms (Extended Data Fig. 1).

At frequency-invariant synapses, the amount of neurotransmitter release scales linearly with the firing frequency, and can thus faithfully encode presynaptic spike rates. Sensorimotor processing in the vestibular system and intensity discrimination in the auditory system have been proposed to operate through a linear rate code[4,27,28]. Understanding the mechanisms involved in frequency-invariant transmission will enable genetic manipulations that could yield fundamental insights into how synaptic computations contribute to circuit function and behaviour.

1. Abbott, L. F., Varela, J. A., Sen, K. & Nelson, S. B. Synaptic depression and cortical gain control. *Science* **275,** 220–224 (1997).
2. Abbott, L. F. & Regehr, W. G. Synaptic computation. *Nature* **431,** 796–803 (2004).
3. MacLeod, K. M., Horiuchi, T. K. & Carr, C. E. A role for short-term synaptic facilitation and depression in the processing of intensity information in the auditory brain stem. *J. Neurophysiol.* **97,** 2863–2874 (2007).
4. Bagnall, M. W., McElvain, L. E., Faulstich, M. & du Lac, S. Frequency-independent synaptic transmission supports a linear vestibular behavior. *Neuron* **60,** 343–352 (2008).
5. Turecek, J., Jackman, S. L. & Regehr, W. G. Synaptic specializations support frequency-independent Purkinje cell output from the cerebellar cortex. *Cell Reports* **17,** 3256–3268 (2016).
6. Zucker, R. S. & Regehr, W. G. Short-term synaptic plasticity. *Annu. Rev. Physiol.* **64,** 355–405 (2002).
7. Jackman, S. L., Turecek, J., Belinsky, J. E. & Regehr, W. G. The calcium sensor synaptotagmin 7 is required for synaptic facilitation. *Nature* **529,** 88–91 (2016).
8. Cook, D. L., Schwindt, P. C., Grande, L. A. & Spain, W. J. Synaptic depression in the localization of sound. *Nature* **421,** 66–70 (2003).
9. Galarreta, M. & Hestrin, S. Frequency-dependent synaptic depression and the balance of excitation and inhibition in the neocortex. *Nat. Neurosci.* **1,** 587–594 (1998).
10. Brenowitz, S., David, J. & Trussell, L. Enhancement of synaptic efficacy by presynaptic GABA(B) receptors. *Neuron* **20,** 135–141 (1998).
11. McElvain, L. E., Faulstich, M., Jeanne, J. M., Moore, J. D. & du Lac, S. Implementation of linear sensory signaling via multiple coordinated mechanisms at central vestibular nerve synapses. *Neuron* **85,** 1132–1144 (2015).
12. Zhou, H. *et al.* Cerebellar modules operate at different frequencies. *eLife* **3,** e02536 (2014).
13. Liu, H. *et al.* Synaptotagmin 7 functions as a Ca^{2+}-sensor for synaptic vesicle replenishment. *eLife* **3,** e01524 (2014).
14. Wen, H. *et al.* Distinct roles for two synaptotagmin isoforms in synchronous and asynchronous transmitter release at zebrafish neuromuscular junction. *Proc. Natl Acad. Sci. USA* **107,** 13906–13911 (2010).
15. Luo, F. & Sudhof, T. C. Synaptotagmin-7-mediated asynchronous release boosts high-fidelity synchronous transmission at a central synapse. *Neuron* **94,** 826–839, (2017).
16. Müller, M., Goutman, J. D., Kochubey, O. & Schneggenburger, R. Interaction between facilitation and depression at a large CNS synapse reveals mechanisms of short-term plasticity. *J. Neurosci.* **30,** 2007–2016 (2010).
17. Wu, D. *et al.* Postsynaptic synaptotagmins mediate AMPA receptor exocytosis during LTP. *Nature* **544,** 316–321 (2017).
18. Jackman, S. L., Beneduce, B. M., Drew, I. R. & Regehr, W. G. Achieving high-frequency optical control of synaptic transmission. *J. Neurosci.* **34,** 7704–7714 (2014).
19. Borst, J. G. The low synaptic release probability *in vivo. Trends Neurosci.* **33,** 259–266 (2010).
20. Arenz, A., Silver, R. A., Schaefer, A. T. & Margrie, T. W. The contribution of single synapses to sensory representation *in vivo. Science* **321,** 977–980 (2008).
21. Kuenzel, T., Borst, J. G. & van der Heijden, M. Factors controlling the input-output relationship of spherical bushy cells in the gerbil cochlear nucleus. *J. Neurosci.* **31,** 4260–4273 (2011).
22. Sugita, S. *et al.* Synaptotagmin VII as a plasma membrane Ca^{2+} sensor in exocytosis. *Neuron* **30,** 459–473 (2001).
23. Bakken, T. E. *et al.* A comprehensive transcriptional map of primate brain development. *Nature* **535,** 367–375 (2016).
24. Lein, E. S. *et al.* Genome-wide atlas of gene expression in the adult mouse brain. *Nature* **445,** 168–176 (2007).
25. Jackman, S. L. & Regehr, W. G. The mechanisms and functions of synaptic facilitation. *Neuron* **94,** 447–464 (2017).
26. Brandt, D. S., Coffman, M. D., Falke, J. J. & Knight, J. D. Hydrophobic contributions to the membrane docking of synaptotagmin 7 C2A domain: mechanistic contrast between isoforms 1 and 7. *Biochemistry* **51,** 7654–7664 (2012).
27. Robinson, D. A. The use of control systems analysis in the neurophysiology of eye movements. *Annu. Rev. Neurosci.* **4,** 463–503 (1981).
28. Sullivan, W. E. & Konishi, M. Segregation of stimulus phase and intensity coding in the cochlear nucleus of the barn owl. *J. Neurosci.* **4,** 1787–1799 (1984).

METHODS

Animals and viruses. All mice were handled in accordance with NIH guidelines and protocols approved by the Harvard Medical Area Standing Committee on Animals. Syt7 knockout mice[29] (Jackson Laboratory) and wild-type littermates of either sex were used. Statistical tests were not used to predetermine sample size. Unless stated otherwise, the experiments were not randomized. In Figs 3a–g, 4d–g and Extended Data Figs 2, 7, 8, all experiments were performed blind to genotype and virus identity. In Figs 1, 2 and Extended Data Figs 3–6, experiments were initially performed blind but blinding was abandoned after the initial rounds of experiments because genotypes could easily be identified from physiology alone. AAV2/1-hSyn-hChR2(H134R)–EYFP was obtained from the University of Pennsylvania Vector Core. AAV2/1-hSyn-hChR2(H134R)–EYFP–2A-Syt7 was obtained from the Boston Children's Virus Core. Plasmid sequences are available upon request.

Stereotaxic surgeries were performed on P16–18 Syt7 knockout mice anaesthetized with ketamine/xylazine (100/10 mg/kg) supplemented with isoflurane (1–4%). Viruses were injected through glass capillary needles using a Nanoject II (Drummond) mounted on a stereotaxic apparatus (Kopf). Three injections were made in the right cerebellar cortex: 1.0, 1.5, 2.0 mm lateral, 1 mm posterior from lambda, 0.2–0.3 mm depth; 300–500 nl virus suspension was delivered to each site at a rate of 100 nl per min, and the needle was retracted 5–10 min after injection. Analgesic (buprenorphine 0.05 mg/kg) was administered subcutaneously for 48 h post-surgery.

Slice preparation. Acute slices were prepared from mice of both sexes (P21–32 unless otherwise indicated). Mice were killed 12–14 days after AAV injections. Animals were anaesthetized with ketamine/xylazine (100/10 mg/kg) and transcardially perfused with solution composed of (in mM): 110 choline Cl, 2.5 KCl, 1.25 NaH_2PO_4, 25 $NaHCO_3$, 25 glucose, 0.5 $CaCl_2$, 7 $MgCl_2$, 3.1 Na pyruvate, 11.6 Na ascorbate, 0.002 (R)-CPP, 0.005 NBQX, oxygenated with 95% O_2/5% CO_2, kept at 35 °C. For DCN recordings, a cut was made down the midline of the hindbrain, and the cut face of each side was glued to the slicing chamber to generate sagittal slices. For the vestibular nuclei, a cut was made down the midbrain between the cerebellum and cortex and glued to the slicing chamber to generate coronal slices. Two hundred and fifty micrometre thick sections were made on a Leica 1200S vibratome and were then transferred to a holding chamber with ACSF containing (in mM): 127 NaCl, 2.5 KCl, 1.25 NaH_2PO_4, 25 $NaHCO_3$, 25 glucose, 1.5 $CaCl_2$, 1 $MgCl_2$, and allowed to recover at 35 °C for at least 20 min before cooling to room temperature.

Electrophysiology. All experiments were performed at 34–35 °C with a flow rate of 3–5 ml/min. The recording ACSF had the same composition as the incubation ACSF unless otherwise stated. Recordings were made primarily in the dentate and interposed nuclei of the DCN. Large diameter (>15 μm) neurons were selected for recording as previously described[5]. For DCN recordings, borosilicate electrodes (1–2 MΩ) were filled with internal solution consisting (in mM) of: 110 CsCl, 10 HEPES, 10 TEA-Cl, 1 $MgCl_2$, 4 $CaCl_2$, 5 EGTA, 20 Cs-BAPTA, 2 QX314, 0.2 D600, pH 7.3. Cells were held at −30 to −40 mV in the presence of 5 μM NBQX to block AMPA receptors, 2.5 μM (R)-CPP to block NMDA receptors, 1 μM strychnine to block glycine receptors, and 1 μM CGP 55845 to block $GABA_B$ receptors. A glass monopolar stimulus electrode (2–3 MΩ) filled with ACSF was placed in the white matter surrounding the DCN to activate PC axons.

To study vestibular afferents, recordings were made from cells in the magnocellular medial vestibular nucleus. Recording electrodes (1.5–2 MΩ) were filled with (in mM): 150 Cs-gluconate, 3 CsCl, 10 HEPES, 0.5 EGTA, 3 MgATP, 0.5 NaGTP, 5 Tris-phosphocreatine and 5 Na-phosphocreatine; pH 7.2. Cells were held at −60 mV in the presence of 100 μM picrotoxin or 5 μM SR-95531 to block $GABA_A$ receptors, 2.5 μM (R)-CPP to block NMDA receptors, 1 μM strychnine to block glycine receptors, and 1 μM CGP 55845 to block $GABA_B$ receptors. A concentric bipolar electrode was placed in the expansion of the vestibulocochlear nerve as it reaches the dorsal brainstem, adjacent to the lateral vestibular nucleus. To prevent poor fibre recruitment or entrainment of local circuit elements, trains with EPSCs composed of multi-phasic rise or decay phases were excluded from analysis. For trains in low Ca_e, EPSCs became very small. In some cases, 5 μM NBQX was washed in at the end of experiments and traces in the presence of NBQX were subtracted to remove stimulus artefacts.

Trains of 100 stimuli (5–150 Hz, randomized), followed by 100 stimuli at 100 Hz, were applied every 20–30 s for vestibular and PC synapses. For 500-stimulus trains at 100 Hz, trials were collected every 60 s. Extracellular stimulation of axons became unreliable after 500 stimuli. For all recordings, only the capacitance roughly equivalent to the cell body was compensated (5 pF), and series resistance (1–6 MΩ) was compensated up to 80%. Experiments were discarded if series resistance changed by 30%. Experiments were discarded if fibres could not be consistently recruited, as assessed by major discrete changes observed in PSC amplitude during trains, or if the PSC amplitude never reached steady state during trains. Liquid

junction potentials were left unsubtracted. In low Ca_e experiments, total divalents were kept constant by elevating external Mg. Experiments using the low affinity $GABA_A$ receptor antagonist TPMPA were performed as previously described[5].

Analysis. Recordings were collected using a Multiclamp 700B (Molecular Devices) in Igor Pro (Wavemetrics) sampled at 20 kHz and filtered at 4 kHz. All data were analysed using custom-written scripts in Matlab (Mathworks). Stimulus artefacts were blanked for clarity. IPSC amplitudes during trains were measured from averaged traces of 3–10 trials as the peak evoked current, with a baseline measured 2 ms before stimulus onset. During high-frequency trains, IPSCs did not fully decay before subsequent stimuli. Baselines in this case were measured by extrapolating a single exponential fit from the previous IPSC (Extended Data Fig. 6). Trains from rest typically reached steady-state after 10–20 stimuli, and the steady-state was measured as the average IPSC size of the 40th to 60th stimuli. Charge transfer was calculated as the product of steady-state IPSC size and stimulation frequency, and normalized to the charge transfer of 10 Hz stimulation. All data are presented as means ± s.e.m. unless otherwise indicated. In some cases error bars are occluded by markers. Statistical significance was assessed using unpaired two-tailed Student's t-test or one-way ANOVA with Tukey's post-hoc test unless otherwise noted. A subset of the data from wild-type Syt7 littermates (∼50%) in Fig. 1 and Fig. 2d (middle) has been presented previously[5].

Optogenetics. It was impossible to reliably stimulate PC axons with prolonged trains at high frequency (>50 Hz) using optical stimulation alone (ChR2–H134R or Chronos). We therefore used ChR2–YFP to identify labelled fibres that were then stimulated electrically. In this approach, optical stimulation of axons expressing ChR2–YFP could occlude electrical stimulation of the same fibres, presumably because of the refractory period of the action potential. By contrast, if electrically stimulated fibres did not express ChR2–YFP, electrically evoked responses could not be occluded by optical stimulation, and combined stimulation was equivalent to the linear sum of optical and electrical activation alone. PC boutons expressing ChR2–YFP were stimulated by pulses of 473 nm light (0.5–1 ms, 160 mW/mm²) from an LED (Thorlabs) through a 60× objective producing an 80-μm diameter spot of light over the cell body. A stimulus electrode was placed in the white matter and converging PC axons were located as in other experiments. Randomized trials of single optical, electrical, or closely timed (0–2 ms) paired optical and electrical stimuli were applied every 5 s. When more than 70% of the electrically evoked component could be occluded by optical stimulation, and could be consistently recruited, those fibres were then activated using high-frequency electrical stimulation. Following electrical trains, occlusion trials were performed again to confirm that the same set of fibres was stimulated throughout all trials. At the end of experiments, a low concentration of SR-95531 (300–800 nM) was washed in and occlusion trials were again repeated to ensure occlusion was not the result of poor voltage clamp. In a subset of experiments, light pulses were also delivered over the stimulus electrode instead of the cell body, producing similar results.

Immunohistochemistry. Mice of both sexes (P21–32 unless otherwise indicated) were anaesthetized with ketamine/xylazine (100/10 mg/kg) and transcardially perfused with PBS followed by 4% paraformaldehyde (PFA) in PBS. To determine the expression of Syt7, Syt2, calbindin and VGAT specifically in PCs, we also perfused one mouse (at P43) in which PC synapses were labelled with TdTomato (Pcp2-Cre(Jdhu) × Synaptophysin–TdTomato, Extended Data Fig. 2). Brains were removed and post-fixed in PFA overnight. Sagittal sections of the cerebellum or coronal sections of the brainstem (50 μm) were then permeabilized (0.2% triton X-100 in PBS) for 10 min and blocked for 1 h (4% normal goat serum in 0.1% triton X-100) at room temperature. Slices were then incubated overnight at 4 °C with primary antibodies (mouse anti-Syt7 targeting the C2A domain, UC Davis/NIH NeuroMab Facility, clone N275/14, RRID: AB_11030371, 1 μg/ml, 1:100; rabbit anti-calbindin D28K, Millipore Ab1778, 1:200; mouse anti-Syt2, Zirc znp-1, 1:200; guinea-pig anti-VGAT, Synaptic Systems 131004, 1 μg/ml, 1:500; guinea-pig anti-VGLUT2, Synaptic Systems 135404, 1 μg/ml, 1:1,200). To prevent background when co-staining with VGLUT2 and Syt7, Syt7 primary antibodies were applied alone overnight at 4 °C, then VGLUT2 primary antibodies alone for 2 h at room temperature. Following primary antibodies, slices were incubated with secondary antibodies for 2 h at room temperature (anti-rabbit-AlexaFluor488, Abcam ab150077; anti-guinea-pig-AlexaFluor488, Abcam ab150185; anti-mouse-AlexaFluor647, Abcam ab150115). For experiments comparing ages or genotypes, all tissue was stained and processed in parallel. Z-stacks of each sample were collected using an Olympus Fluoview1000 confocal microscope using the same settings across ages and genotypes, and processed identically in ImageJ. For each genotype and age, identical anatomical locations and tissue depth were selected for presentation.

Modelling. In a previous study we modelled the PC–DCN synapse[5]. Models used previously to explain data in young animals[30] were reproduced, but could not fit the data from P21–32 mice[5]. Several other types of models were also attempted but failed to accurately account for data observed in juvenile wild-type mice.

We found that a two-pool model fit all experimental observations[5]. We extended this model to Syt7 knockout mice (Extended Data Fig. 9). In this model there are two pools of vesicles, consisting of, respectively, $N1$ and $N2$ vesicles, with initial probability of release $P1$ and $P2$ and time constants of recovery τ_{R1} and τ_{R2}. $P1$ stays constant whereas $P2$ increases as a result of facilitation, $F2$, which has the frequency dependence that was determined experimentally. All of these parameters were constrained by extensive experimental studies for wild-type mice[5]. Once parameters for wild-type data were determined, $F2$ was set to 0 to model Syt7 knockout mice. Minor adjustments (<15% change) were made to some parameters to fit the data more accurately, with the exception of τ_{R1}, which was reduced by 55% to conform to the observed recovery from depression in Syt7 knockouts (Extended Data Fig. 5). This change in τ_{R1} had a negligible effect on steady-state IPSC amplitudes because Pool 1 still depleted rapidly. Parameters for modelling wild-type mice were: $N1/N2 = 0.35$; $P1 = 0.20$; $\tau_{R1} = 7.7\,\mathrm{s}$; $P2 = 0.025$; $\tau_{R2} = 0.2\,\mathrm{s}$; $F2 = 0.04$; $\tau_{Fdeact} = 0.1\,\mathrm{s}$. Parameters for modelling Syt7 knockout mice were: $N1/N2 = 0.36$; $P1 = 0.23$; $\tau_{R1} = 3.5\,\mathrm{s}$; $P2 = 0.025$; $\tau_{R2} = 0.2\,\mathrm{s}$; $F2 = 0$.

Data availability. The data, computational models and analysis scripts that support the findings are available upon reasonable request from the corresponding author.

29. Chakrabarti, S. *et al.* Impaired membrane resealing and autoimmune myositis in synaptotagmin VII-deficient mice. *J. Cell Biol.* **162,** 543–549 (2003).
30. Telgkamp, P., Padgett, D. E., Ledoux, V. A., Woolley, C. S. & Raman, I. M. Maintenance of high-frequency transmission at Purkinje to cerebellar nuclear synapses by spillover from boutons with multiple release sites. *Neuron* **41,** 113–126 (2004).
31. Sakaba, T. & Neher, E. Calmodulin mediates rapid recruitment of fast-releasing synaptic vesicles at a calyx-type synapse. *Neuron* **32,** 1119–1131 (2001).
32. Dittman, J. S. & Regehr, W. G. Calcium dependence and recovery kinetics of presynaptic depression at the climbing fiber to Purkinje cell synapse. *J. Neurosci.* **18,** 6147–6162 (1998).
33. Stevens, C. F. & Wesseling, J. F. Activity-dependent modulation of the rate at which synaptic vesicles become available to undergo exocytosis. *Neuron* **21,** 415–424 (1998).
34. Wang, L. Y. & Kaczmarek, L. K. High-frequency firing helps replenish the readily releasable pool of synaptic vesicles. *Nature* **394,** 384–388 (1998).
35. Yang, H. & Xu-Friedman, M. A. Impact of synaptic depression on spike timing at the endbulb of Held. *J. Neurophysiol.* **102,** 1699–1710 (2009).
36. McElvain, L. E., Bagnall, M. W., Sakatos, A. & du Lac, S. Bidirectional plasticity gated by hyperpolarization controls the gain of postsynaptic firing responses at central vestibular nerve synapses. *Neuron* **68,** 763–775 (2010).
37. Telgkamp, P. & Raman, I. M. Depression of inhibitory synaptic transmission between Purkinje cells and neurons of the cerebellar nuclei. *J. Neurosci.* **22,** 8447–8457 (2002).
38. Atluri, P. P. & Regehr, W. G. Delayed release of neurotransmitter from cerebellar granule cells. *J. Neurosci.* **18,** 8214–8227 (1998).
39. Hefft, S. & Jonas, P. Asynchronous GABA release generates long-lasting inhibition at a hippocampal interneuron-principal neuron synapse. *Nat. Neurosci.* **8,** 1319–1328 (2005).
40. Lu, H. W. & Trussell, L. O. Spontaneous activity defines effective convergence ratios in an inhibitory circuit. *J. Neurosci.* **36,** 3268–3280 (2016).
41. Trommershäuser, J., Schneggenburger, R., Zippelius, A. & Neher, E. Heterogeneous presynaptic release probabilities: functional relevance for short-term plasticity. *Biophys. J.* **84,** 1563–1579 (2003).
42. Thanawala, M. S. & Regehr, W. G. Determining synaptic parameters using high-frequency activation. *J. Neurosci. Methods* **264,** 136–152 (2016).
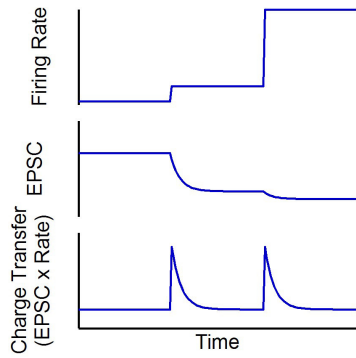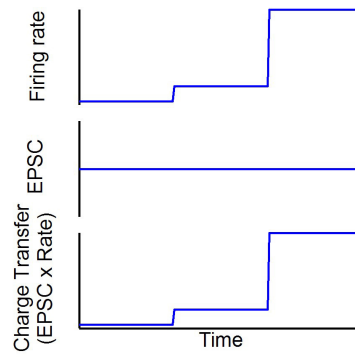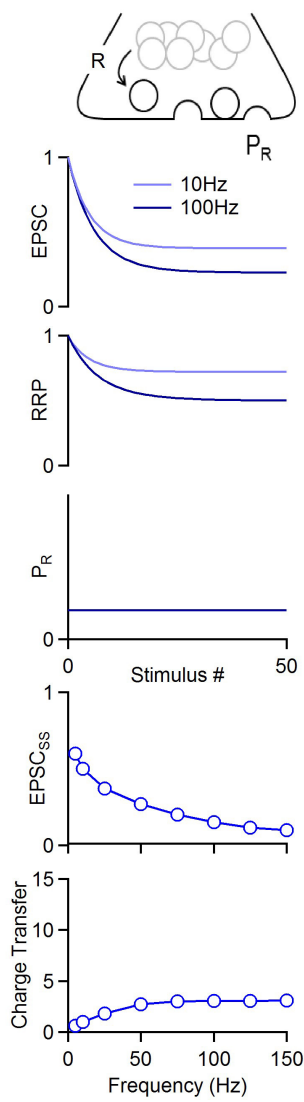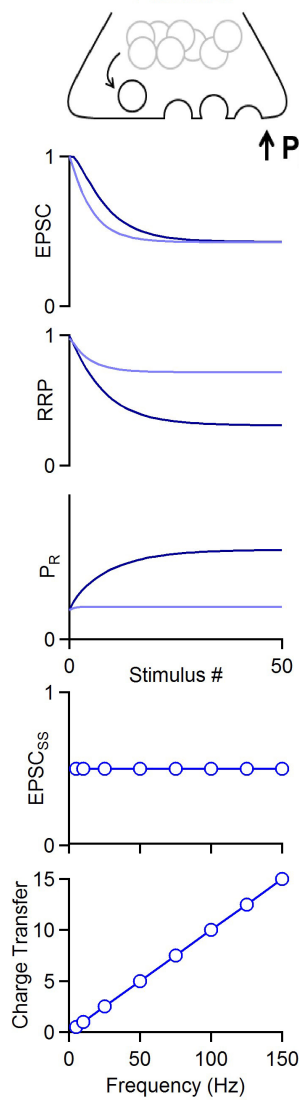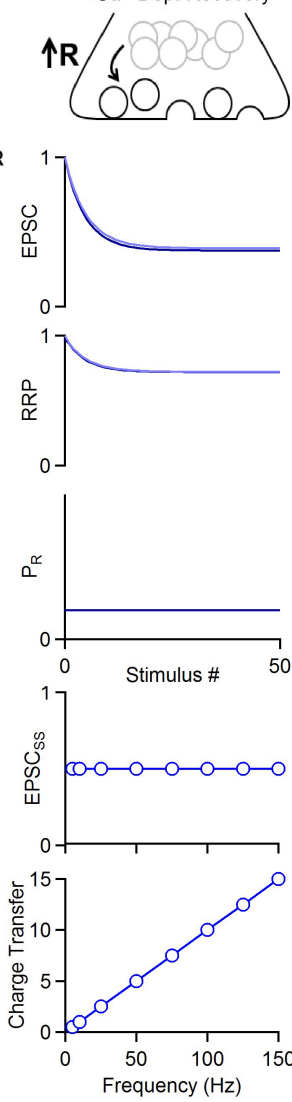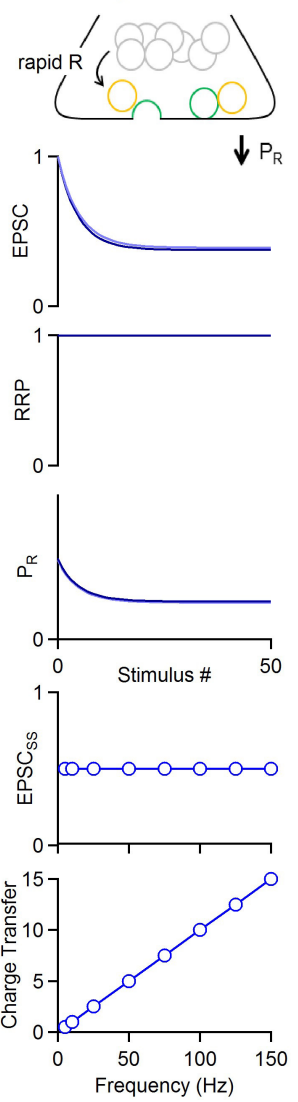
Extended Data Figure 1 | See next page for caption.

Extended Data Figure 1 | Functions and possible mechanisms of frequency-invariant synapses. Short-term plasticity at synapses can be tuned to perform different computations. **a**, Many synapses in the brain undergo short-term depression that is use-dependent: elevations in presynaptic firing rate (top) result in more profound depression of postsynaptic currents (EPSCs, middle). The charge transfer that ultimately drives postsynaptic firing increases rapidly with presynaptic firing, but short-term depression of the synapse reduces charge transfer back to a similar steady state. Thus, short-term depression is suited to convey temporal information about changes in presynaptic firing. **b**, Some synapses maintain constant strength across firing frequencies (top, middle). Charge transfer at these synapses can therefore reliably reflect the absolute rate of presynaptic firing. **c**, Typical depressing synapses can be well-approximated by intrinsic synaptic properties alone. Synapses have a limited number of vesicles in the readily releasable pool (RRP). High-frequency presynaptic activity depletes the RRP until it can be replenished at some rate (R). Less recovery occurs as the interval between stimuli is reduced, thereby leading to an increase in depletion during high-frequency stimulation. **d**–**f**, Other synaptic features must operate in order to generate frequency-invariant synapses, and several possibilities have been proposed. **d**, One way of making transmission frequency-invariant would be to balance depletion with facilitation[3,5] (Extended Data Fig. 9). Activating a mechanism of short-term facilitation with high-frequency stimulation increases P_R, releasing more vesicles from the RRP. The increase in release results in steady-state transmission that is consistent across the physiological firing range. **e**, Another way of generating a frequency-invariant synapse would be to have a rapid, calcium-dependent increase in R[31–35]. When the presynaptic frequency is elevated, presynaptic calcium and the rate of replenishment are increased to maintain the same RRP size regardless of activation frequency. However, this cannot explain the frequency invariance of PC and vestibular synapses, where recovery from depression is insensitive to stimulation frequency in juvenile animals[5,36]. **f**, In this proposed model[36], each release site can hold two vesicles, but only one can be released per stimulus (green, releasable; orange, non-releasable). Vesicle replenishment to each release site is very rapid, and release is limited by a decrease in P_R. Decreases in P_R are independent of stimulation frequency. The high replenishment rate and additional vesicle per release site results in very little vesicle depletion, and responses are instead shaped by decreases in P_R that are constant across frequencies. Another possibility is that a synapse could have very low P_R to limit vesicle depletion at each release site, but still maintain synaptic strength by having a very large number of release sites (not shown). However, such a mechanism would require an extremely large number of release sites, and is inconsistent with the depression present at PC and vestibular synapses. Finally, postsynaptic mechanisms of short-term plasticity, such as receptor saturation and desensitization, could also contribute to frequency-invariant transmission (not shown). These mechanisms are unlikely to contribute to frequency invariance at PC and vestibular synapses because frequency-independent transmission is unaltered when saturation and desensitization are minimized by competitive low-affinity postsynaptic receptor antagonists[4,5].
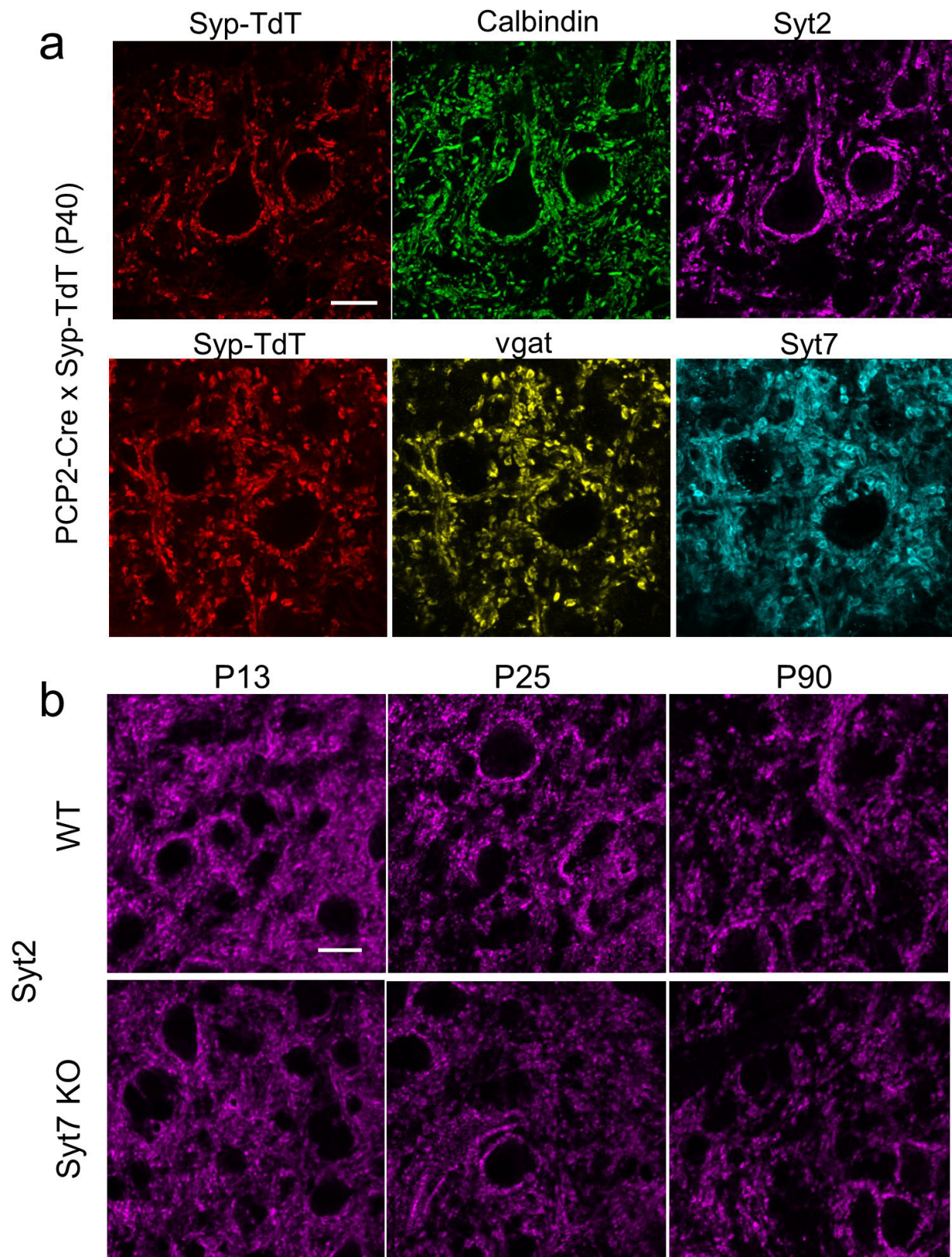
Extended Data Figure 2 | Expression and localization of synaptic proteins to PC synapses in the DCN. To determine whether Syt7 was present at PC synapses in the DCN, we compared immunohistochemical labelling in mice expressing synaptophysin–TdTomato (Syp–TdT) specifically in PCs (PCP2–Cre × Syp–TdT). **a**, Syp–TdT could be observed in boutons surrounding neurons in the DCN (upper left). Immunolabelling of calbindin could be seen both in PC boutons labelled with Syp–TdT, and throughout the length of PC axons traversing the DCN (upper middle). Syt2 was also highly expressed in PC boutons, with most Syt2 puncta co-localizing with Syp–TdT (upper right). We found that the vast majority of inhibitory synapses labelled by VGAT were Syp–TdT positive, suggesting that most inhibitory input to the DCN arises from PCs (lower middle). Syt7 was also prominent in PC boutons labelled by Syp–TdT, but with less punctate expression compared to Syt2 or VGAT. Scale bar, 15 μm. **b**, The expression of Syt2 was stable across development, and showed no prominent differences in intensity between wild-type and Syt7 knockout mice. Scale bar, 20 μm.
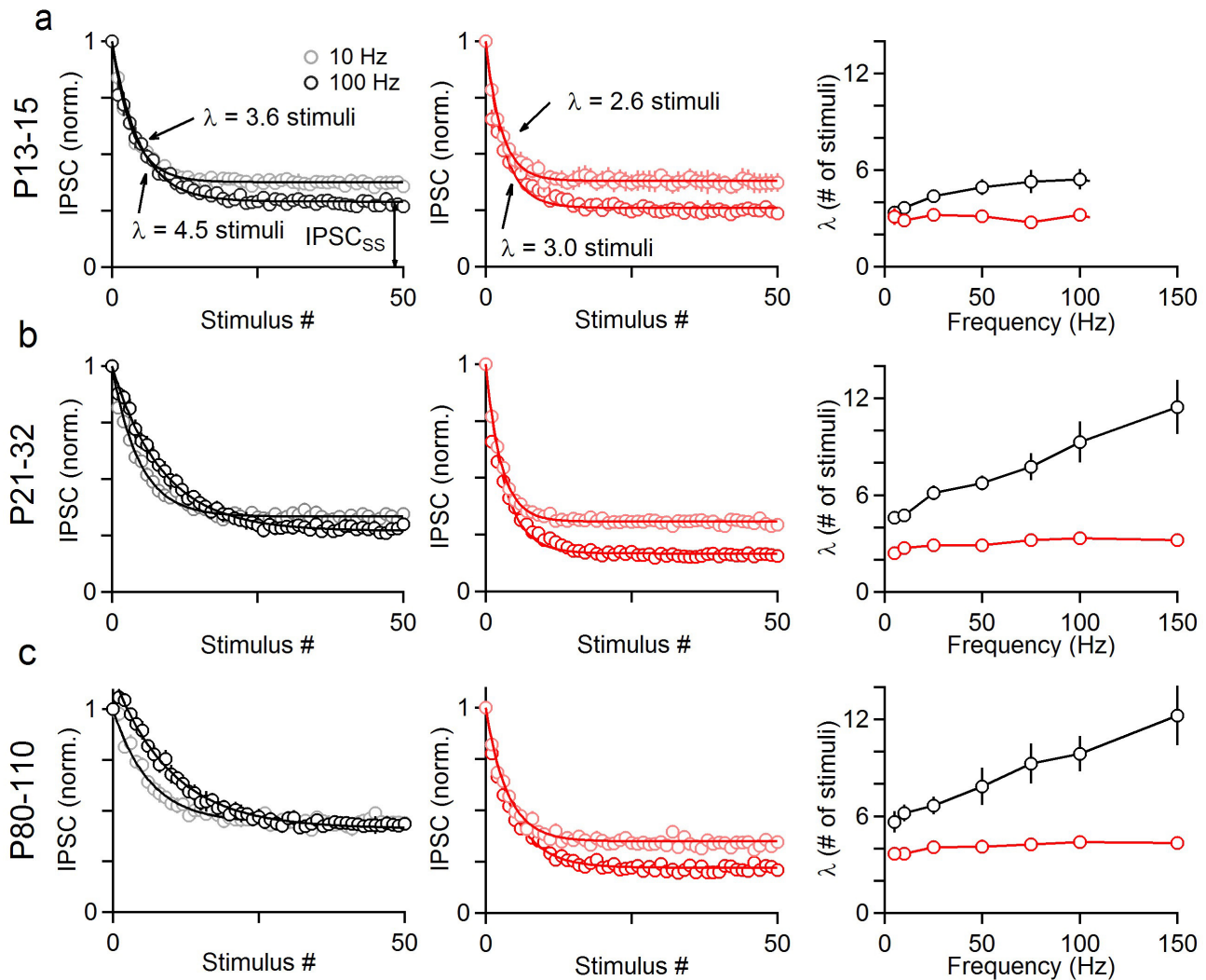
Extended Data Figure 3 | Alterations in short-term depression at PC to DCN synapses in Syt7 knockout mice are consistent with the predicted consequences of eliminating facilitation. High-frequency stimulation of the PC–DCN synapse leads to depressing IPSCs that can be approximated by the equation $IPSC = IPSC_{SS} + (1 - IPSC_{SS})e^{-S/\lambda}$, where S is the stimulus number, $IPSC_{SS}$ is the steady-state IPSC amplitude, and λ is the exponential decay constant. **a**, Average normalized IPSC amplitude for 10- and 100-Hz trains and fits in P13–15 wild-type (left) and Syt7 knockout (middle) mice. λ is plotted as a function of stimulation frequency (right). **b**, As in **a**, but for P21–32 mice. **c**, As in **a**, but for P80–110 mice. According to a model of the PC–DCN synapse, both depression and facilitation are present, but depletion of the readily releasable pool dominates and leads to depression during high-frequency stimulation[5]. In wild-type mice, λ is prolonged in a frequency-dependent manner, and it has been hypothesized that this arises from short-term facilitation that is more prominent as the stimulus frequency is increased. In young animals, when Syt7 expression is low (Fig. 1c), λ is weakly modulated by stimulation frequency. The prolongation of λ is more prominent in juveniles and adults. In the absence of Syt7, λ is not frequency dependent at any age. These observations are consistent with an age-dependent increase in Syt7 expression in wild-type mice leading to an age-dependent increase in facilitation, which in turn leads to age-dependent increases in the frequency dependence of λ. Data are mean ± s.e.m. Number of experiments shown in Extended Data Table 1.
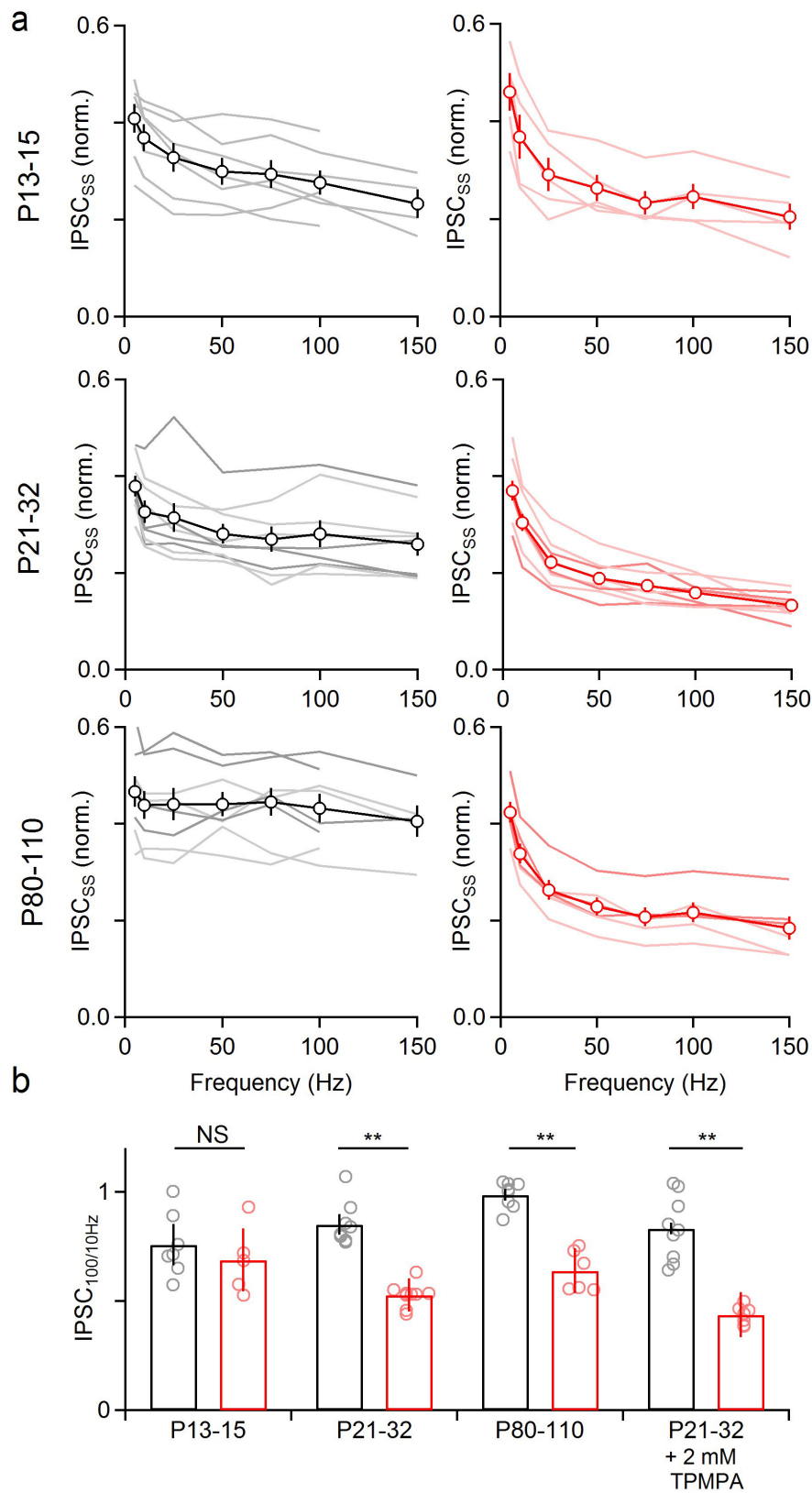
Extended Data Figure 4 | The frequency dependence of synaptic strength is consistent for different cells for a given age and genotype. a, The steady-state IPSC amplitude as a function of frequency for each cell analysed (thin lines) and averages (markers) for each genotype and age. Normalized steady-state IPSC amplitudes across frequencies are plotted for wild-type (left) and Syt7 knockout mice (right) at P13–15, P21–32, and P80–110. **b**, Ratio of the steady-state IPSC amplitudes at 100 Hz divided by steady-state amplitudes at 10 Hz is summarized for different ages of wild-type and Syt7 knockout mice, and in P21–32 mice in the presence of the low-affinity $GABA_A$ receptor antagonist TPMPA (2 mM, far right). Data from young animals are consistent with previous reports[5,30,37]. **$P < 0.01$, unpaired two-tailed Student's t-test. Data are mean ± s.e.m. Number of experiments shown in Extended Data Table 1.
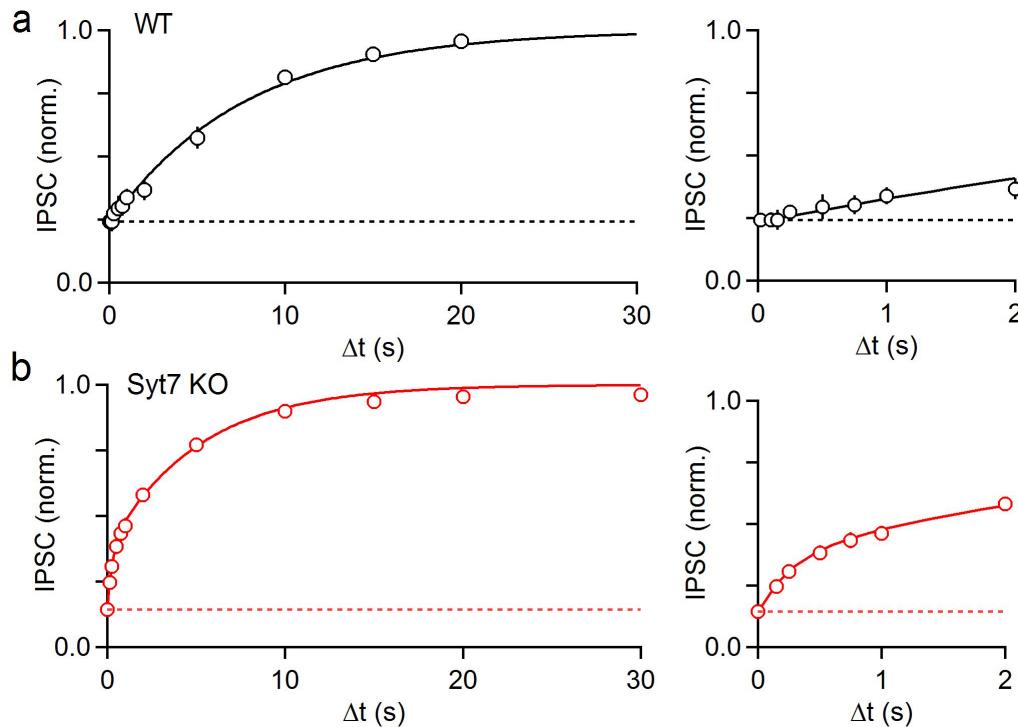
Extended Data Figure 5 | Altered recovery from depression in Syt7 knockout mice cannot account for the loss of frequency invariance at the PC–DCN synapse in Syt7 knockout mice at P21–32. It has been shown previously that the loss of Syt7 in hippocampal cultures slows recovery from depression[13]. If recovery from depression were slower in Syt7 knockouts, it could partially explain the reduction of sustained transmission at high frequencies. We therefore examined recovery from depression at PC–DCN synapses. One hundred stimuli at 100 Hz were followed by a single stimulus after an interval. This was repeated for many trials and a range of time intervals. Experiments were performed in wild-type (**a**) and Syt7 knockout (**b**) mice. **a**, PC–DCN synapses recovered slowly with a single exponential of 7.7 s (left). **b**, In Syt7 knockout mice, recovery could not be approximated by a single exponential but was well approximated by a double exponential with time constants of 280 ms and 5.1 s. These findings indicate that a slowed recovery from depression does not occur in Syt7 knockout mice and thus does not contribute to the reduced steady-state responses in Syt7 knockout mice. The rapid time constant of recovery from depression that is apparent in Syt7 knockout mice is consistent with the prediction of a model of the PC–DCN synapse in which the decay of facilitation obscures this rapid phase of recovery in wild-type mice[5] (Extended Data Fig. 9). The role of Syt7 in recovery from depression at the PC–DCN synapse differs from that at cultured hippocampal synapses, where calcium-dependent recovery from depression relies on Syt7, and recovery from depression is slowed in the absence of Syt7[13]. Data are mean ± s.e.m. Number of experiments shown in Extended Data Table 1.
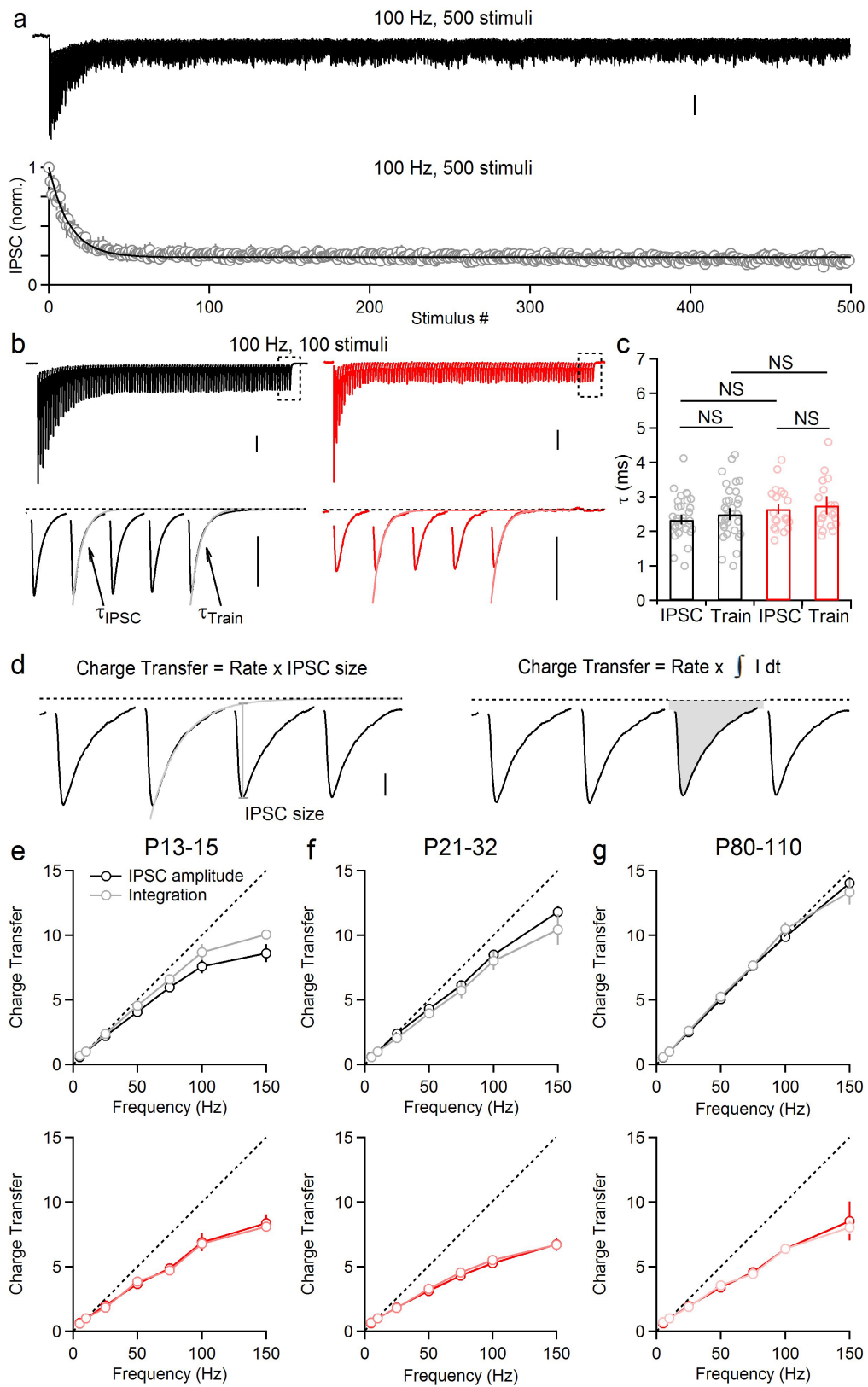
**Extended Data Figure 6** | See next page for caption.

Extended Data Figure 6 | Release from PCs to DCN neurons is sustained, fast and synchronous. a, PCs fire at high rates spontaneously *in vivo*. We therefore examined whether the PC–DCN synapse could sustain transmission for prolonged high-frequency activation. **a**, Example of prolonged stimulation of PC axons (500 stimuli, 100 Hz), average of four trials (top), and average across cells (bottom) and fit with the equation $IPSC = IPSC_{SS} + (1 − IPSC_{SS})e^{−S/\lambda}$ as in Extended Data Fig. 3. Vertical scale bar, 1 nA. **b–g**, At some synapses, asynchronous release becomes more prominent with prolonged high-frequency stimulation[14,15,38,39]. At these synapses, fast synchronous release can be seen riding on top of a slowly decaying current that is, in part, mediated by asynchronous release. We therefore investigated whether asynchronous release contributes to transmission during trains at the PC–DCN synapse. **b**, Example trains of 100 stimuli at 100 Hz from a wild-type (black) and Syt7 knockout (red) mouse. Responses evoked by the entire train are plotted (top) and regions within the dashed boxes are shown on an expanded scale (bottom). We measured the average decay time constant of IPSCs during the train (average IPSC number 50–99, τ_{IPSC}), and for the last IPSC in the train (τ_{Train}). IPSCs were well fit by a single exponential decay with similar values of τ. This indicates that asynchronous release is not prominent at this synapse. Vertical scale bars, 0.5 nA; dashed line indicates baseline before the train. **c**, Average decay time for IPSCs during the train, and for the last IPSC in the train to decay back to baseline measured before the onset of stimulation. No significant differences were found between wild-type τ_{IPSC} and wild-type τ_{train} ($P = 0.36$), Syt7 knockout τ_{IPSC} and Syt7 knockout τ_{train} ($P = 0.71$), wild-type τ_{IPSC} and Syt7 knockout τ_{IPSC} ($P = 0.23$), or wild-type τ_{train} and Syt7 knockout τ_{train} ($P = 0.48$), unpaired two-tailed student's t-test. **d**, Charge transfer was measured in two different ways to isolate different components of release. The average incremental IPSC amplitude was multiplied by the stimulation rate (left), or traces were integrated and multiplied by stimulation rate (right). The average charge transfer as a function of stimulation frequency, calculated either by IPSC amplitude, or by integration, for young (**e**, P12–15), juvenile (**f**, P21–32), and adult (**g**, P80–110) wild-type and Syt7 knockout mice is shown. Data are mean ± s.e.m. Number of experiments shown in Extended Data Table 1.
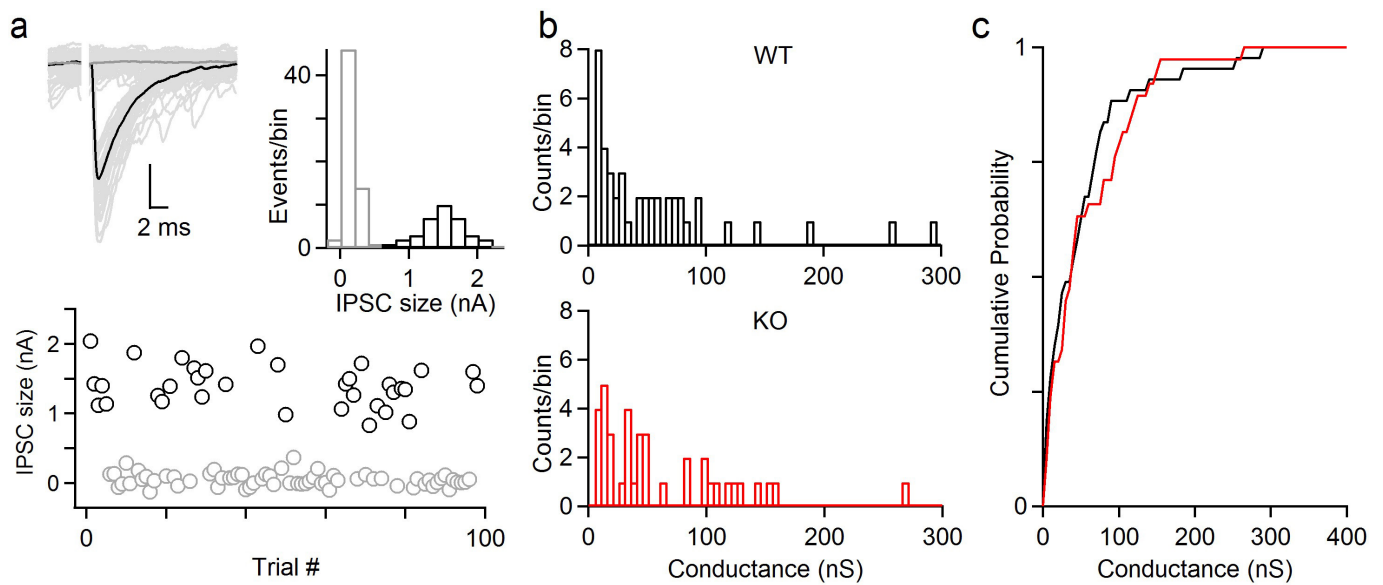
Extended Data Figure 7 | Single-fibre conductances are not elevated in Syt7 knockout mice (P21–32). Single PC axons provide powerful inhibition on their postsynaptic targets in the DCN, and can be identified by their all-or-nothing nature. If the loss of Syt7 caused elevations in P_R, it would be expected to increase the strength of unitary fibre inputs. Experiments were done using minimal stimulation to determine the amplitudes of single PC–DCN inputs. **a**, The stimulus was adjusted so that, at a constant intensity, synaptic inputs were activated approximately half the time in a stochastic manner. This is shown for 100 superimposed traces (left), along with average of failures (thick grey) and average of successes (thick black), for the amplitude histogram for the events recorded in that cell (middle), and for the IPSC amplitude as a function of trial number (bottom). Vertical scale bar, 0.5 nA. **b**, Amplitude histogram of single-fibre conductances for wild-type (black) and Syt7 knockout mice (red). **c**, Cumulative amplitude histograms of single-fibre conductances. No significant difference was found between wild-type (black) and Syt7 knockout mice (red). $P = 0.43$, Kolmogorov–Smirnov test. Number of experiments shown in Extended Data Table 1.
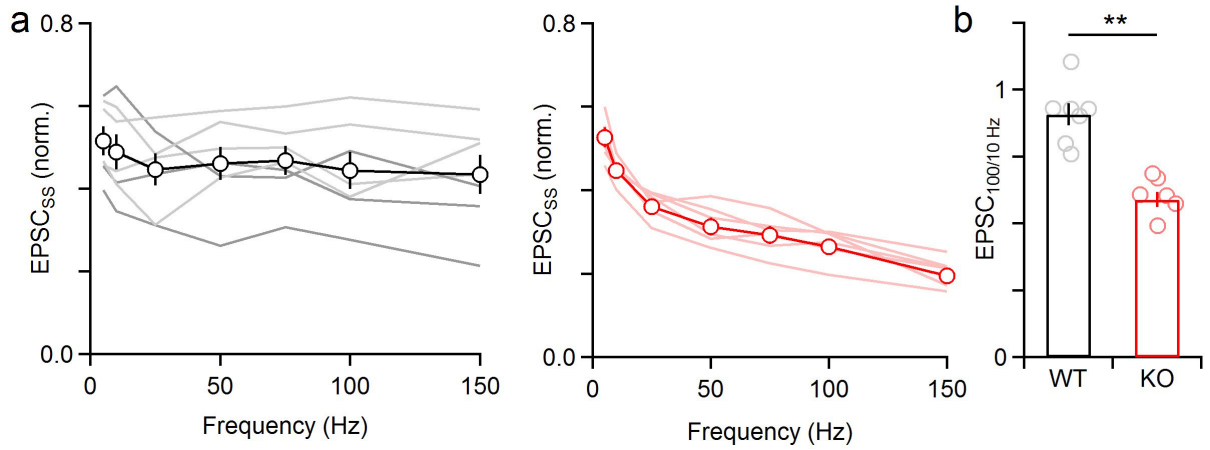
Extended Data Figure 8 | The frequency invariance of synaptic strength is consistent in the MVNm. a, The steady-state EPSC size as a function of stimulation frequency for each cell analysed (thin lines) and averages (markers) for wildtype (left, black) and Syt7 knockouts (red, right). **b,** Ratio of the steady-state EPSC amplitudes at 100 Hz divided by steady-state amplitudes at 10 Hz is summarized for vestibular synapses in wildtype and Syt7 knockouts. **$P < 0.01$, unpaired two-tailed Student's t-test. Data are mean ± s.e.m. Number of experiments shown in Extended Data Table 1.
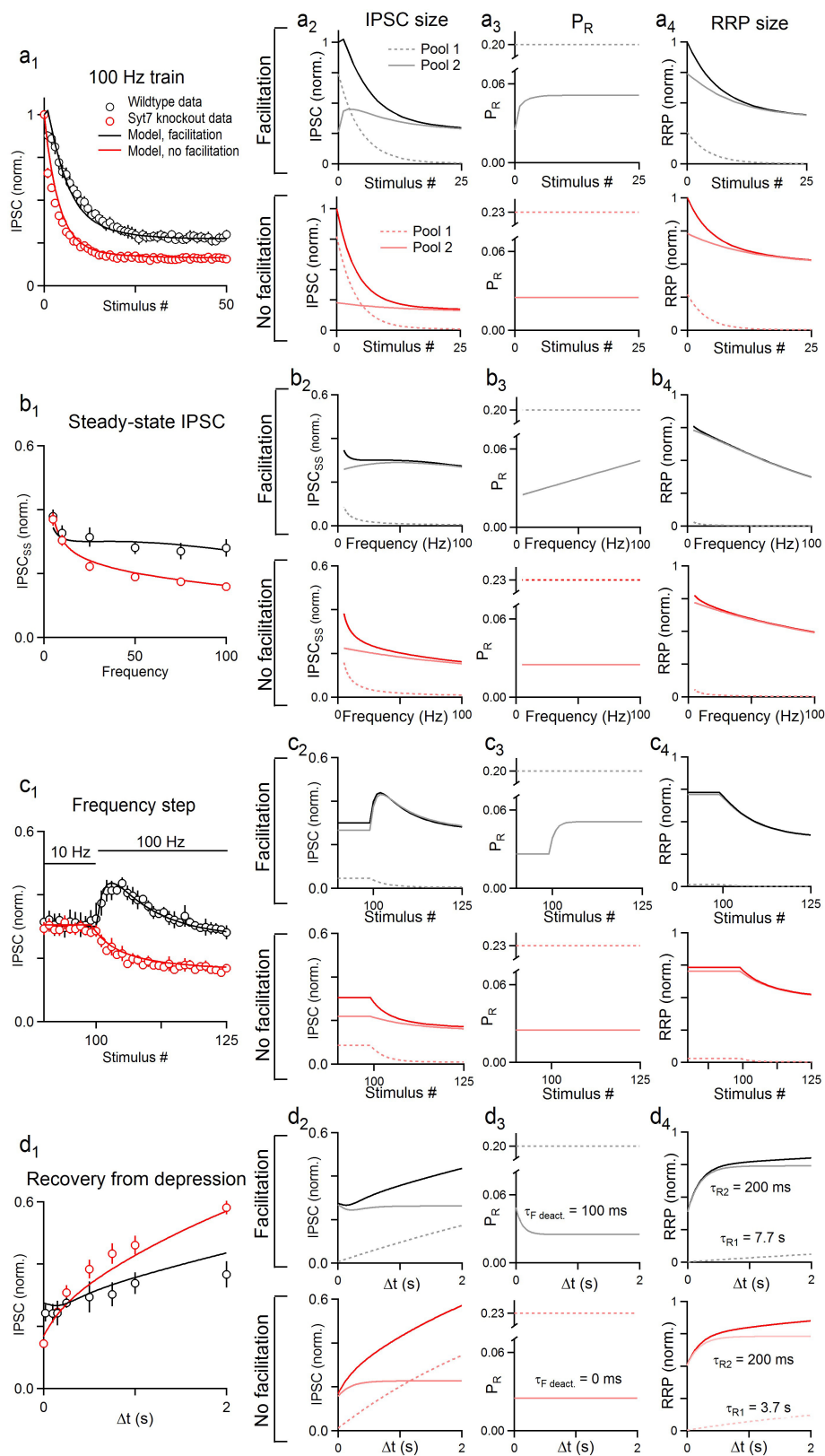
Extended Data Figure 9 | See next page for caption.

Extended Data Figure 9 | A model of the PC–DCN synapse indicates that eliminating facilitation can explain the loss of frequency-invariant transmission and other synaptic changes observed in Syt7 knockout mice. We extended a previously described model of PC–DCN synapses to explore transmission in Syt7 knockout mice[5]. The model consists of two pools of vesicles. Pool 1 vesicles have a high release probability and are replenished slowly. Pool 2 vesicles have a low initial release probability that increases with facilitation (in wild-type animals only), and replenish rapidly. The existence of multiple vesicle pools has been proposed at several types of synapses[40–42]. The model was constrained by many experiments and in the simplest configuration could account for all experimental observations[5]. The model is compared to data from wild-type and Syt7 knockout mice (a_1–d_1). The contribution of each pool and its properties (IPSC size a_2–d_2, release probability P_R a_3–d_3, and readily releasable pool size RRP a_4–d_4) are also shown for each experiment. **a**, During high-frequency stimulation in wild-type mice ($a_{1–2}$, black), Pool 1 primarily contributes to depression seen during the onset of stimulation, but is strongly depleted during sustained firing (a_2, dashed grey). Pool 2 facilitates and maintains release at steady-state ($a_{2–3}$, solid grey). We modelled Syt7 knockout mice by removing facilitation (a_3, red). When facilitation was eliminated, steady-state transmission was reduced during high-frequency stimulation because fewer vesicles were released from Pool 2 (a_4, light red). **b**, In the model of wild-type synapses, the magnitude of facilitation increased with stimulation frequency (b_3, grey), allowing more of the RRP of Pool 2 (RRP2) to be released at high frequencies, resulting in similar IPSC amplitude across frequencies ($b_{1–2}$, black). When facilitation was removed (b_3, red), transmission was no longer frequency invariant, because fewer vesicles were released at high frequencies ($b_{1,4}$, red). **c**, When the frequency of stimulation was stepped from 10 to 100 Hz, a transient enhancement was observed in wild-type mice (c_1, black markers). In the model, this transient enhancement is mediated by facilitation of Pool 2 (c_3, grey). Facilitation is weakly activated by 10 Hz stimulation, but increases when stepping to 100 Hz stimulation. As more vesicles are released, RRP2 is partially depleted and the IPSC amplitude depresses, ultimately reaching steady-state levels that are similar to those reached during 10 Hz stimulation. When facilitation is removed, no transient enhancement occurs, and the IPSC amplitude simply depresses ($c_{1–2}$, red). **d**, The model is also able to explain recovery from depression. In wild-type mice, a single slow recovery is observed (d_1, black markers) because the decay of facilitation obscures the rapid recovery of RRP2 ($d_{3–4}$, τ_{Fdeact}). When facilitation is removed, this rapid component of recovery is unmasked ($d_{1–2}$, red). The known role of Syt7 in facilitation, and the fact that the many alterations in synaptic responses in Syt7 knockout animals are explained by eliminating facilitation in this model, support the importance of Syt7-mediated facilitation in frequency-invariant transmission.

Extended Data Table 1 | Number of electrophysiological recordings from wild-type and Syt7 knockout mice

Figure	Experiment	Age	Genotype	Cells	Animals
Figure 1e-f, Extended Data 3a, 4a, 6e	Trains (5-150 Hz)	P13-15	wildtype	7	3
			Syt7 knockout	5	2
Figure 1e-f, Figure 3h Extended Data 3b, 4a, 6f	Trains (5-150 Hz)	P21-32	wildtype	9	8
			Syt7 knockout	9	8
Figure 1e-f, Extended Data 3c, 4a, 6g	Trains (5-150 Hz)	P80-110	wildtype	8	5
			Syt7 knockout	6	2
Extended Data 4b	Trains (5-150 Hz) in 2 mM TPMPA	P21-32	wildtype	9	6
			Syt7 knockout	7	5
Extended Data 5	Recovery from depression (100 Hz)	P21-32	wildtype	6	5
			Syt7 knockout	6	4
Extended Data 6a	Long train (500 stimuli, 100 Hz)	P21-32	wildtype	4	2
Extended Data 6a	IPSC kinetics (τ_{IPSC}, τ_{train})	P21-32	wildtype	32	22
			Syt7 knockout	12	8
Extended Data 7	Single PC fibers	P21-32	wildtype	44 (# fibers)	6
			Syt7 knockout	37 (# fibers)	7
Figure 2a,	0.3 mM Ca_e Trains (100 Hz)	P21-32	wildtype	5	2
			Syt7 knockout	5	3
Figure 2b,c	0.5 mM Ca_e Trains (5-100 Hz)	P21-32	wildtype	6	5
			Syt7 knockout	4	3
Figure 2b,c	1.0 mM Ca_e Trains (5-100 Hz)	P21-32	wildtype	4	3
			Syt7 knockout	4	4
Figure 2d	Frequency step (10-100 Hz)	P13-15	wildtype	4	3
			Syt7 knockout	5	2
Figure 2d	Frequency step (10-100 Hz)	P21-32	wildtype	5	4
			Syt7 knockout	9	8
Figure 2d	Frequency step (10-100 Hz)	P80-110	wildtype	6	5
			Syt7 knockout	6	2
Figure 3b-h	Optical occlusion Frequency step (10-100 Hz) Trains (5-100 Hz)	P21-32	KO+ChR2	7	3
			KO+ChR2+Syt7	5	5
Figure 4c	0.5 mM Ca_e Trains (100 Hz)	P21-32	wildtype	6	3
			Syt7 knockout	6	2
Figure 4d-g Extended Data 8	Frequency step (10-100 Hz) Trains (5-100 Hz)	P21-32	wildtype	7	6
			Syt7 knockout	6	2

nature research

Corresponding author(s):   Wade Regehr

☐ Initial submission ☐ Revised version ☒ Final submission

Life Sciences Reporting Summary

Nature Research wishes to improve the reproducibility of the work that we publish. This form is intended for publication with all accepted life science papers and provides structure for consistency and transparency in reporting. Every life science submission will use this form; some list items might not apply to an individual manuscript, but all fields must be completed for clarity.

For further information on the points included in this form, see Reporting Life Sciences Research. For further information on Nature Research policies, including our data availability policy, see Authors & Referees and the Editorial Policy Checklist.

▶ Experimental design

1. Sample size

Describe how sample size was determined.

> Sample sizes were not predetermined.

2. Data exclusions

Describe any data exclusions.

> Data was only excluded under the criteria listed in the methods.

3. Replication

Describe whether the experimental findings were reliably reproduced.

> Data was collected over a period of a year (Figure 1 and 2) and the results remained consistent over that time. Data was collected by the 2 first authors in independent experiments and the results were similar for both.

4. Randomization

Describe how samples/organisms/participants were allocated into experimental groups.

> This study compares synaptotagmin 7 knockout mice and wildtype littermates; randomization is not applicable.

5. Blinding

Describe whether the investigators were blinded to group allocation during data collection and/or analysis.

> In Figure 3-4, Extended Data Figure 2, 7, 8, all experiments were performed blind to genotype and virus identity. In Figures 1-2, Extended Data Figure 3-6, experiments were initially performed blind but abandoned after initial rounds of experiments because genotypes could easily be identified from physiology alone. This is described in the Methods section.

Note: all studies involving animals and/or human research participants must disclose whether blinding and randomization were used.

6. Statistical parameters

For all figures and tables that use statistical methods, confirm that the following items are present in relevant figure legends (or in the Methods section if additional space is needed).

n/a	Confirmed	
☐	☒	The <u>exact sample size</u> (n) for each experimental group/condition, given as a discrete number and unit of measurement (animals, litters, cultures, etc.)
☐	☒	A description of how samples were collected, noting whether measurements were taken from distinct samples or whether the same sample was measured repeatedly
☐	☒	A statement indicating how many times each experiment was replicated
☐	☒	The statistical test(s) used and whether they are one- or two-sided (note: only common tests should be described solely by name; more complex techniques should be described in the Methods section)
☒	☐	A description of any assumptions or corrections, such as an adjustment for multiple comparisons
☐	☒	The test results (e.g. P values) given as exact values whenever possible and with confidence intervals noted
☐	☒	A clear description of statistics including <u>central tendency</u> (e.g. median, mean) and <u>variation</u> (e.g. standard deviation, interquartile range)
☐	☒	Clearly defined error bars

See the web collection on statistics for biologists for further resources and guidance.

▶ Software

Policy information about availability of computer code

7. Software

Describe the software used to analyze the data in this study.

> Physiology data was analyzed using custom-written scripts in Matlab. As stated in the methods they are available upon request.

For manuscripts utilizing custom algorithms or software that are central to the paper but not yet described in the published literature, software must be made available to editors and reviewers upon request. We strongly encourage code deposition in a community repository (e.g. GitHub). *Nature Methods* guidance for providing algorithms and software for publication provides further information on this topic.

▶ Materials and reagents

Policy information about availability of materials

8. Materials availability

Indicate whether there are restrictions on availability of unique materials or if these materials are only available for distribution by a for-profit company.

> All materials are publicly available, except viruses:
> AAV2/1-hSyn-ChR2-YFP is available at the UPenn Vector Core
> AAV2/1-hSyn-ChR2-YFP-2a-Syt7 was generated at the Boston Children's Vector Core; plasmid sequences are available upon request of the authors as indicated in the Methods.

9. Antibodies

Describe the antibodies used and how they were validated for use in the system under study (i.e. assay and species).

> As indicated in the Methods:
> Mouse anti-Syt7 targeting the C2A domain, NeuroMab clone N275/14
> Rabbit anti-Calbindin D28K, Millipore Ab1778
> Mouse anti-Syt2, Zirc znp-1
> Guinea-pig anti-vgat, Synaptic Systems 131004
> Guinea-pig anti-vglut2, Synaptic Systems 135404
>
> Syt7 antibodies were validated for brain immunohistochemistry as presented in figure 1 using syt7 knockout animals.
> Syt2 antibodies were vailidated for brain immunohistochemistry using syt2 knockout animals (Kobuchey & Schneggenburger, 2010)
> All other antibodies were validated as described by their vendors.

10. Eukaryotic cell lines

a. State the source of each eukaryotic cell line used.

> N/A

b. Describe the method of cell line authentication used.

> N/A

c. Report whether the cell lines were tested for mycoplasma contamination.

> N/A

d. If any of the cell lines used are listed in the database of commonly misidentified cell lines maintained by ICLAC, provide a scientific rationale for their use.

> N/A

▶ Animals and human research participants

Policy information about studies involving animals; when reporting animal research, follow the ARRIVE guidelines

11. Description of research animals

Provide details on animals and/or animal-derived materials used in the study.

> Syt7 knockout animals were obtained from Jackson labs (B6.129S1-Syt7tm1Nan/J), initially generated in the lab of Norma Andrews (Chakrabarti et al. 2003).

Policy information about studies involving human research participants

12. Description of human research participants

Describe the covariate-relevant population characteristics of the human research participants.

> N/A